NASA Contractor Report 172486

ICASE REPORT NO. 84-57

ICASE

MULTIPLE STEADY STATES FOR CHARACTERISTIC INITIAL VALUE PROBLEMS

M. D. Salas

S. Abarbanel

D. Gottlieb

Contract No. NAS1-17070

November 1984

INSTITUTE FOR COMPUTER APPLICATIONS IN SCIENCE AND ENGINEERING
NASA Langley Research Center, Hampton, Virginia 23665

Operated by the Universities Space Research Association

National Aeronautics and
Space Administration

Langley Research Center
Hampton, Virginia 23665

MULTIPLE STEADY STATES FOR CHARACTERISTIC INITIAL VALUE PROBLEMS

M. D. Salas
NASA Langley Research Center

S. Abarbanel and D. Gottlieb
Tel-Aviv University, Tel-Aviv, Israel
and
Institute for Computer Applications in Science and Engineering

Abstract

The time dependent, isentropic, quasi-one-dimensional equations of gas dynamics and other model equations are considered under the constraint of characteristic boundary conditions. Analysis of the time evolution shows how different initial data may lead to different steady states and how seemingly anamolous behavior of the solution may be resolved. Numerical experimentation using time consistent explicit algorithms verifies the conclusions of the analysis. The use of implicit schemes with very large time steps leads to erroneous results.

Research was supported in part by the National Aeronautics and Space Administration under NASA Contract No. NAS1-17070 while the second and third authors were in residence at ICASE, NASA Langley Research Center, Hampton, VA 23665.

INTRODUCTION

Consider a steady, isentropic flow in a dual-throat nozzle with equal throat areas, and assume that the flow is chocked; then it is well known [1] that the flow between the throats can be either completely subsonic or supersonic depending on the initial state of the flow and the path taken to reach the steady state. If we experiment numerically with the above problem using either the isentropic quasi-one-dimensional gas dynamics equation or some "simpler" model equation, then some of the results obtained are rather peculiar.

(1) If the initial data corresponds to sufficiently high supersonic flow (or sufficiently low subsonic flow), then the steady state flow obtained between the two throats is indeed completely supersonic (subsonic).

(2) If the initial data are completely supersonic (or subsonic), but below a certain level (above a certain level), then the steady state flow contains a shock wave connecting the supersonic branch of the solution to the subsonic branch. For the model equations considered, the shock corresponds to an isentropic jump, and its location depends on the initial data.

(3) Results (1) and (2) above are observed when time accurate schemes are used. However, the implicit backwards Euler scheme with large time steps yields steady states that are not reachable through a time accurate path from any class of nontrivial initial conditions. These steady states include not only discontinuous solutions (as observed in [2]), but also unstable smooth solutions.

(4) The numerical treatment of boundary conditions was very important in obtaining the proper results. For example, with central space differencing one may have a stable algorithm that does not converge in time to a steady state if the sonic conditions are invoked in order to supply numerical boundary conditions.

The purpose of this paper is to present our findings, and to provide, where possible, a mathematical explanation of the observed behavior, thereby removing the apparent peculiarities. We will show that the nonuniqueness aspect of the steady state solution is a by-product of the fact that the boundary conditions for the evolution equations are prescribed along characteristic curves. This is true for the dual throat problems due to the sonic conditions imposed at the throats. The model problems were therefore chosen to show this behavior.

In Section 2, we study the model equation

$$\frac{\partial u}{\partial t} + \frac{\partial}{\partial x}\left(\frac{u^2}{2}\right) = u(1 - u).$$

The relevance of this model equation to the quasi-one-dimensional gas dynamical equations is somewhat peripheral. However, it is rich in the number of possible steady solutions that it admits, including unstable continuous and discontinuous solutions. In this section, we set down the proper way to formulate the characteristic boundary conditions for first order quasi-linear hyperbolic equations.

In Section 3, we consider the model equation

$$\frac{\partial u}{\partial t} + \frac{\partial}{\partial x}\left(\frac{u^2}{2}\right) = \sin x \cos x.$$

This model equation has solutions which qualitatively behave as do those of the isentropic dual throat nozzle problem. The simplicity of the model, however, affords a detailed study of the possibilities for anomalous behavior. This model equation will also show us how to quantify such vague terms as sufficiently high (or low) supersonic (subsonic) initial conditions that were mentioned in (1) and (2) above. These results are summarized in Theorems 1 and 2.

In Section 4, a model scalar equation is developed which has all of the interesting physical aspects of the complete isentropic quasi-one-dimensional gas dynamic equations governing the dual throat nozzle problem. To develop this equation, our guideline was to retain the differential equation exhibiting the characteristic boundary condition, and to model the other dependent variable by assuming constant total enthalpy during the time evolution. By comparing the theoretical results of the model equation to numerical calculations for the complete system of equations, this section shows that the proposed single equation is indeed a good model of the complete system. Here, by the "goodness" of the model we mean that all of the important features of the system are retained.

2. FIRST EXAMPLE

Here we consider the scalar hyperbolic partial differential equation:

$$\frac{\partial u}{\partial t} + \frac{\partial}{\partial x}\left(\frac{u^2}{2}\right) = u(1 - u), \qquad 0 \leq x \leq 1, \quad t > 0,$$

$$u(x,0) = g(x). \tag{2.1}$$

For reasons mentioned in the introduction, and to be discussed in detail in Section 4, we are interested in cases that model physical situations in which the boundaries are characteristic. In practice, when (2.1) is solved numerically as a characteristic boundary value problem, the boundary conditions are imposed dynamically as follows:

$$u(0,t) = \begin{cases} 0 \quad \text{if} \quad u(\varepsilon_0,t) > 0 & (\varepsilon_0 = \Delta x) \\ \text{unspecified if} \quad u(\varepsilon_0,t) \leq 0 \end{cases} \tag{2.2a}$$

$$u(1,t) = \begin{cases} 0 \quad \text{if} \quad u(\varepsilon_1,t) < 0 & (\varepsilon_1 = 1 - \Delta x) \\ \text{unspecified if} \quad u(\varepsilon_1,t) \geq 0 \end{cases} \tag{2.2b}$$

There are two families of continuous steady states satisfying (2.1) and the analytical versions of (2.2):

$$u = 0 \tag{2.3}$$

$$u = 1 - e^{\eta - x} \qquad (0 \leq \eta \leq 1). \tag{2.4}$$

The stability theory of ordinary differential equations applied to the characteristic equation $du/dt = u(1 - u)$ easily shows that the steady state solution $u = 0$ is unstable.

There are also weak solutions connecting various branches (different η's) of (2.4). These discontinuous solutions are unstable as will be demonstrated now: let

$$u_L = 1 - e^{\eta_1} e^{-x} \tag{2.5}$$

be a steady state corresponding to $\eta = \eta_1$,

$$u_R = 1 - e^{\eta_2} e^{-x} \tag{2.6}$$

be another branch.

Since we want to rule out "expansion shock," i.e., discontinuities that do not obey the 'entropy law', we will consider only the case of $1 \geq \eta_2 > \eta_1 \geq 0$, although the analysis is unchanged if $\eta_2 < \eta_1$. For a steady state shock we require $u_L(x_S) + u_R(x_S) = 0$. This determines the shock location, x_S, to be

$$x_S = \ell n \frac{e^{\eta_1} + e^{\eta_2}}{2} . \tag{2.7}$$

We now ask, what will be the shock speed, $\dot{x}_S = \frac{1}{2}(u_L + u_R)$, if x_S is perturbed to $x_S + \varepsilon$? Upon substituting the perturbed shock position in (2.5) and (2.6), we get for the new shock speed

$$\frac{u_L + u_R}{2} = 1 - e^{-\varepsilon} \approx \varepsilon + 0(\varepsilon^2). \tag{2.8}$$

Thus, if $\varepsilon > 0$ ($\varepsilon < 0$) the shock will move to the right (left), showing that the solution with a shock is not stable.

We have thus shown that in the steady state we need consider only the smooth solutions in (2.4). We will now demonstrate that these solutions are reachable from initial data. The demonstration is first done for the case $\eta = 0$, $g(x) > 0$ for all $x > 0$, and $g(0) = 0$:

Consider the problem, (2.1), and let

$$g(x) = b(1 - e^{-x}), \qquad b > 0. \tag{2.9}$$

The solution to this problem is readily verified as

$$u(x,t) = b\,\frac{1 - e^{-x}}{e^{-t} + b(1 - e^{-t})}\,. \tag{2.10}$$

Clearly, as $t \to \infty$, $u(x,t) \to 1 - e^{-x}$, which is a proper steady state.

Suppose now $g(x)$ is not a multiple of the steady state but is a general initial condition still satisfying $g(0) = 0$, $g(x) > 0$. The characteristic equations are

$$\frac{dx}{dt} = u \tag{2.11}$$

$$\frac{du}{dt} = u(1 - u) \tag{2.12}$$

From (2.12) one gets

$$u = \frac{g(\xi)}{g(\xi) + \big(1 - g(\xi)\big)e^{-t}} \tag{2.13}$$

where $\xi = \xi(x,t)$ is the origin of the characteristic passing through x and t. By inserting (2.13) in (2.11) and integrating again along the characteristic, we get the following implicit relation between ξ, x and t:

$$e^{x-\xi-t} = [g(\xi) + (1 - g(\xi))e^{-t}] \tag{2.14}$$

or, upon rearranging

$$g(\xi) = \frac{e^{x-\xi} - 1}{e^{t} - 1} . \tag{2.15}$$

The argument is now as follows: $x - \xi$ is finite $(0 \leq x-\xi < 1)$, and thus as $t \to \infty$, $g(\xi) \to 0$, but $g(\xi) \to 0$ only for $\xi \to 0$. Hence, for any finite x, as t increases, $g(\xi)$ takes the large time asymptotic form of

$$g(\xi) \sim \frac{e^{x} - 1}{e^{t} - 1} \qquad (t \gg 1). \tag{2.16}$$

Substituting (2.16) in (2.13) we get

$$u(x,t) \sim \frac{1 - e^{-x}}{1 - e^{-t}} \qquad (t \gg 1). \tag{2.17}$$

Thus, as $t \to \infty$, $u(x,t) \to 1 - e^{-x}$ regardless of the detailed form of the initial data.

For other types of initial data (e.g., $g(x) = 0$ for some $x = x_0$) the proof is the same with $\eta = x_0$ and the coordinate x transformed to $\bar{x} = x - x_0$.

If $g(x)$ has several simple zeros then the interval $0 \leq x \leq 1$ is subdivided by the zeros. Their relative locations will determine the proper

η. In particular, if $g(x)$ is a periodic function, $g(x_j) = 0$, with $x_j = \frac{jx}{N}$, $j = 0,1\cdots,N$, then

$$\eta = x_N = 1$$

if

$$\text{(i)} \quad \operatorname{sgn} g'(0) = \operatorname{sgn} g'(1) > 0$$

or (2.18a)

$$\text{(ii)} \quad \operatorname{sgn} g'(0) = -\operatorname{sgn} g'(1) < 0$$

and

$$\eta = x_{N-1}$$

if

$$\text{(i)} \quad \operatorname{sgn} g'(0) = \operatorname{sgn} g'(1) < 0$$

or (2.18b)

$$\text{(ii)} \quad \operatorname{sgn} g'(0) = -\operatorname{sgn} g'(1) > 0,$$

(where primes denote differentiation with respect to the independent variable). In summary, this example demonstrates the richness of possible steady state solutions:

(1) There is an unstable smooth solution, $u = 0$;

(2) there are unstable discontinuous solutions;

(3) there is a one-parameter family of smooth steady states,

$$u = 1 - e^{\eta - x}$$

with the value of the parameter depending <u>only</u> on the initial data, a direct consequence of the problem having characteristic boundary values.

It is interesting to note that if the right-hand side of equation (2.1) is taken to be $u(u-1)$, instead of $u(1-u)$, then there is only one possible stable steady state solution satisfying the boundary conditions (2.2), namely

$$u = 0.$$

Note that this was one of the unstable solutions of the previous case.

2.1 NUMERICAL RESULTS FOR THE FIRST EXAMPLE

2.1.1 Explicit Form

The conservative, upwind, first order scheme of Engquist-Osher (E-O), [3] is used to approximate the hyperbolic system of conservation laws represented by

$$\frac{\partial u}{\partial t} + \frac{\partial}{\partial x}\left(\frac{u^2}{2}\right) = h(x,u) \tag{2.19}$$

where h is a source term. Let u_i^n represent the discrete value of u at $t^n = n\Delta t$ and $x_i = i\Delta x$. The explicit, E-O scheme for equation (2.19) is,

$$u_i^{n+1} = u_i^n - \frac{1}{2}\frac{\Delta t}{\Delta x}\left[\frac{1}{2}(1 - \delta_{i+1})(u_{i+1}^n)^2 + \delta_i(u_i^n)^2 - \frac{1}{2}(1 + \delta_{i-1})(u_{i-1}^n)^2\right]$$

$$+ h(i\Delta x, u_i^n)\Delta t \tag{2.20}$$

where the switch function δ_i is defined by

$$\delta_i = \begin{cases} 0 & u_i^n = 0 \\ \dfrac{u_i^n}{|u_i^n|} & u_i^n \neq 0. \end{cases} \tag{2.21}$$

As usual, Δt satisfies the Courant-Friedrichs-Lewy condition,

$$\Delta t \leq \frac{\Delta x}{\max|u_i^n|}, \tag{2.22}$$

and $\Delta x = L/100$, where L is the length of the interval of interest. For the explicit E-O scheme convergence was established according to the criterion

$$\max_i|u_i^{n+1} - u_i^n| < 1. \times 10^{-3}. \tag{2.23}$$

The relation given by equation (2.23) is equivalent to requiring the steady state operator of (2.20) to be less than 10^{-3}. Figure 1 compares the exact and computed steady states for equation (2.1) with initial conditions*

$$g(x) = -\sin 2\pi x. \tag{2.24}$$

Note that the steady state satisfies the condition (2.18bi), and that the initial and steady state solution is such that no boundary conditions are

---

*Note that, because of the first order accuracy of the Enquish-Osher scheme, Figure 1 shows a slight discrepancy between the analytic and numerical solution. The same problem run with $\Delta x = 1/1000$ gives results that, on the scale of Figure 1, are indistinguishable from the analytic results. This comment holds for all other numerical experiments, where, in order to save computer time, we used 100 mesh points.

imposed at either end of the interval. The same steady state is also obtained with

$$g(x) = -x(x-1)(x - \frac{1}{2}). \tag{2.25}$$

Figure 2 compares the exact and computed steady states for initial conditions

$$g(x) = \sin 2\pi x. \tag{2.26}$$

The steady result is in agreement with the condition (2.18ai).

2.1.2 Implicit Form

The slow convergence to steady state characteristic of explicit schemes has stimulated research into various acceleration techniques. One of the most promising avenues for acceleration consists of recasting the discrete equation in implicit form. If we define the increment in time of u by

$$\Delta u_i = u_i^{n+1} - u_i^n, \tag{2.27}$$

then the E-O scheme in implicit form is

$$\frac{1}{2}(1 - \delta_{i+1})u_{i+1}^n \Delta u_{i+1} + \left(\frac{\Delta x}{\Delta t} + \delta_i u_i^n - (\frac{\partial h}{\partial u})_i^n \Delta x\right)\Delta u_i - \frac{1}{2}(1 + \delta_{i-1})u_{i-1}^n \Delta u_{i-1}$$

$$= -\frac{1}{2}\left[\frac{1}{2}(1 - \delta_{i+1})(u_{i+1}^n)^2 + \delta_i(u_i^n)^2 - \frac{1}{2}(1 + \delta_{i-1})(u_{i-1}^n)^2\right] + h(i\Delta x, u_i^n)\Delta x, \tag{2.28}$$

where δ_i is defined as before by equation (2.21). To obtain equation (2.28), terms of order Δu_i^2 and higher are neglected. It is easy to see, by comparing equations (2.20) and (2.28), that the right-hand side of equation (2.28) is the steady state operator. For the implicit E-O scheme convergence was established by requiring that the steady state operator be less than 10^{-5} at all mesh points.

Figure 3 shows the steady state solution obtained using the implicit E-O scheme with

$$g(x) = \sin 2\pi x \tag{2.29}$$

and using infinite Courant number, $\left(\frac{1}{\Delta t} = 0\right)$. The steady state obtained with the implicit form of the scheme corresponds to one of the unstable solutions of equation (2.1). The stable solution, for $g(x)$ corresponding to equation (2.29), was shown in Figure 2. The peculiar behavior of the implicit algorithm at large Courant numbers is further demonstrated in Figure 4 for

$$g(x) = - x(x - 1)(x - \tfrac{1}{2}) \tag{2.30}$$

and infinite Courant number. For this case, the steady state reached by (2.28) consists of a combination of stable and unstable steady, piecewise solutions of equation (2.1).

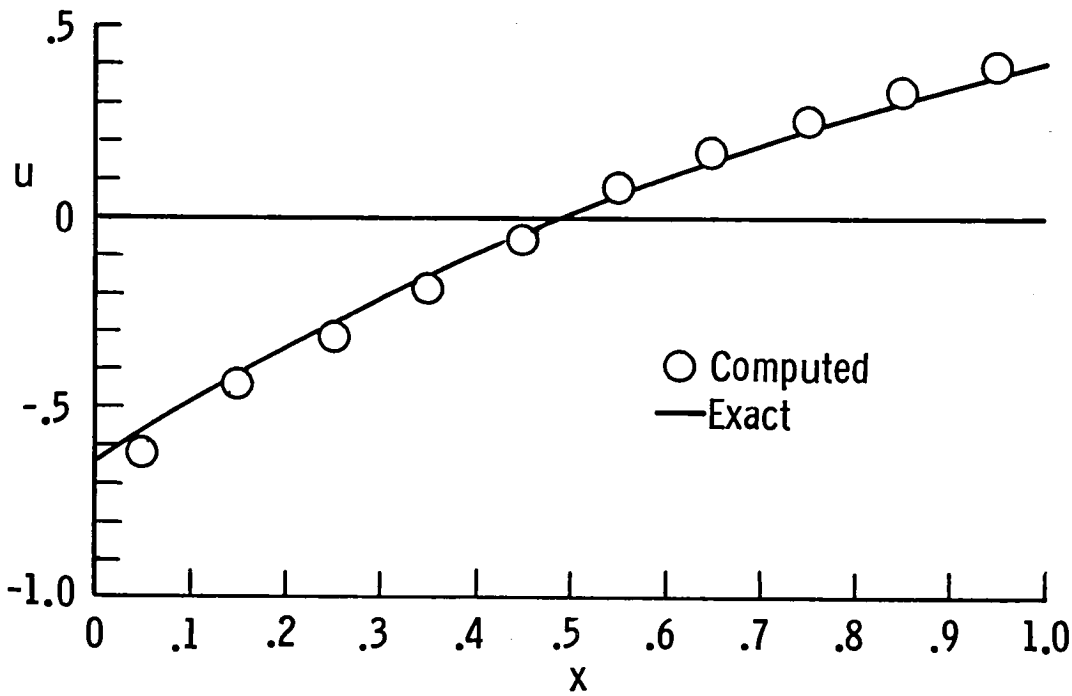

Figure 1. Exact and computed steady states for equation (2.1) with initial conditons (2.24) using a time accurate scheme.

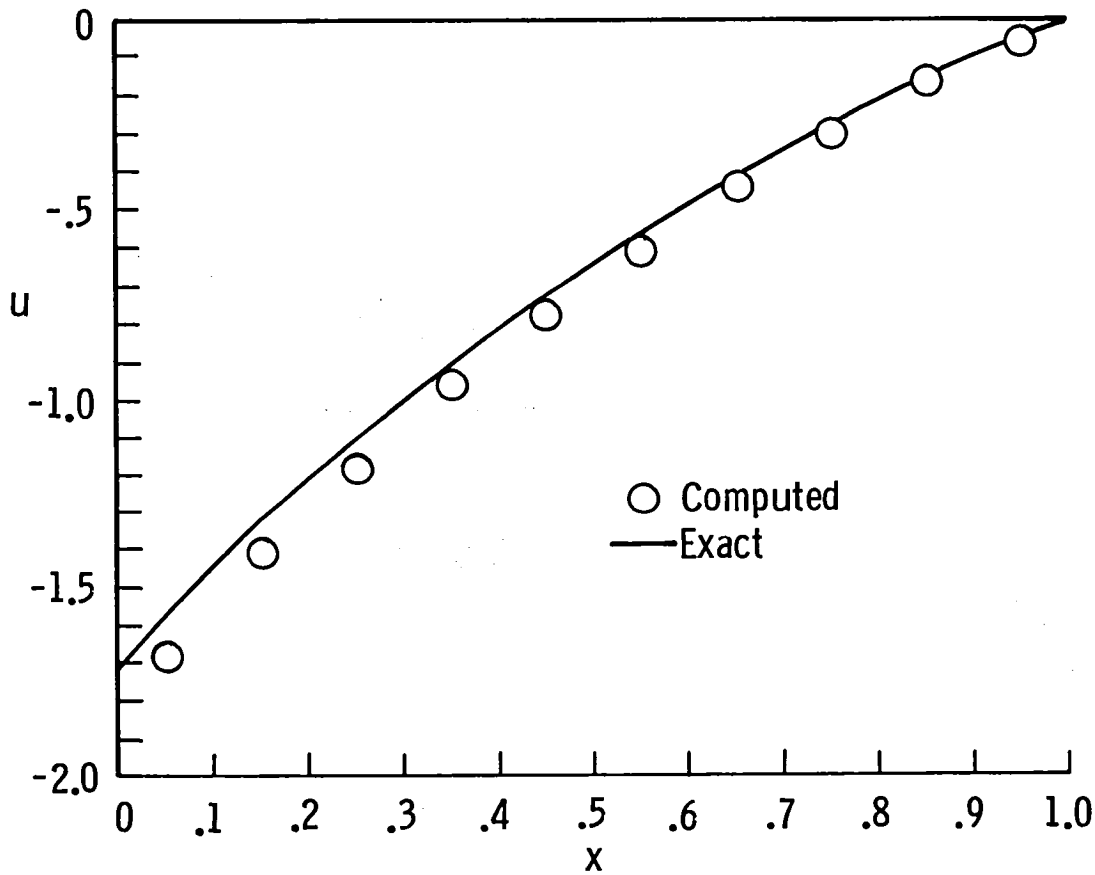

Figure 2. Exact and computed steady states for equation (2.1) with initial conditions (2.26) using a time accurate scheme.

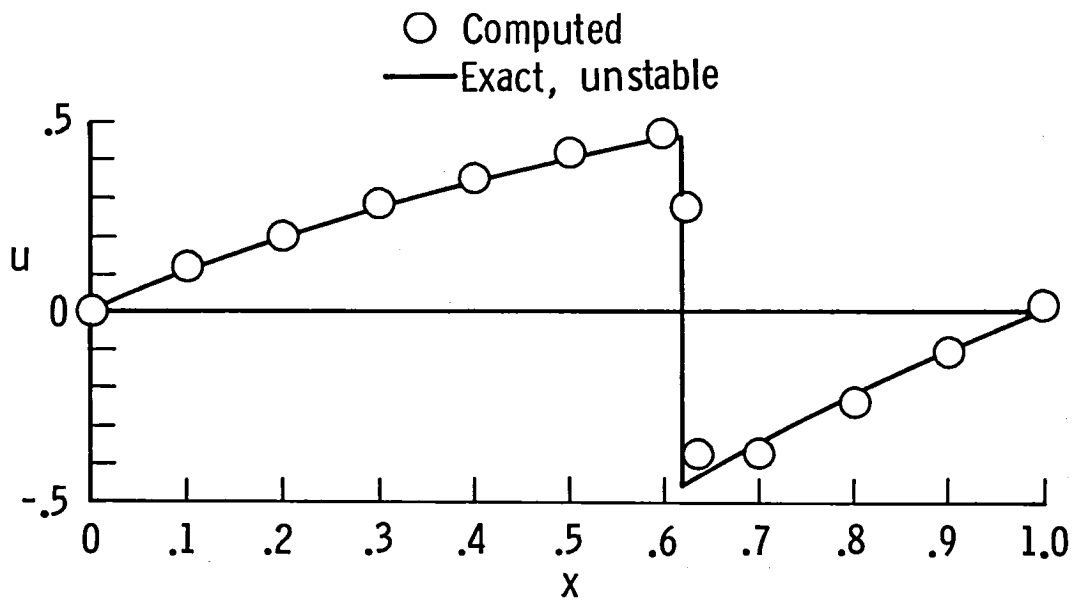

Figure 3. Exact and computed unstable steady states for equation (2.1) with initial conditions (2.29) using an implicit scheme with large Courant number.

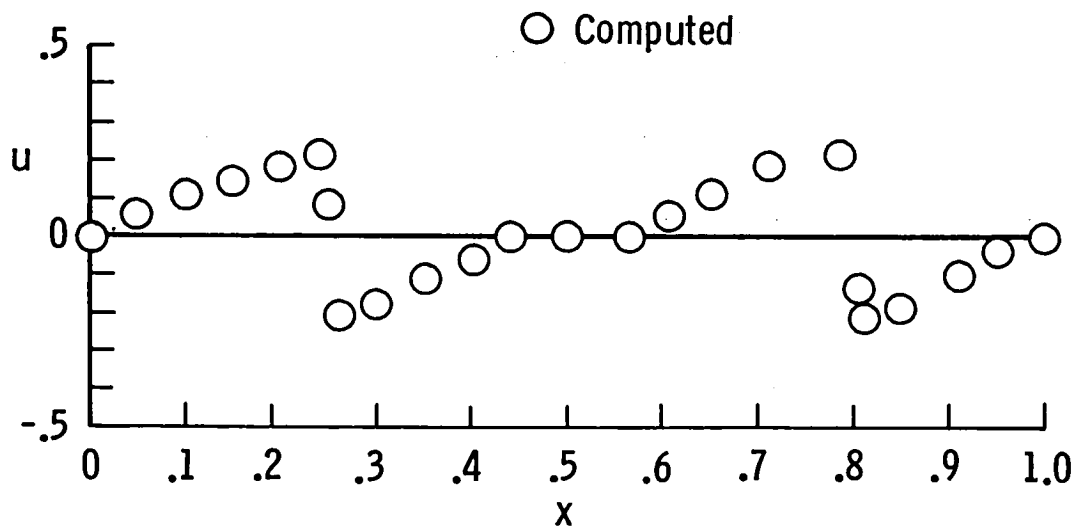

Figure 4. Computed steady state for equation (2.1) with initial conditions (2.30) using an implicit scheme with large Courant number.

3. SECOND EXAMPLE

We now shift our attention to another advection problem. The steady states of this problem will have a completely different nature than of those found in the previous example.

The partial differential equation under consideration is

$$\frac{\partial u}{\partial t} + \frac{\partial}{\partial x}\left(\frac{u^2}{2}\right) = \sin x \cos x, \qquad 0 \leq x \leq \pi, \quad t > 0 \tag{3.1}$$

$$u(x,0) = g(x), \qquad g(0) = g(\pi) = 0.$$

with boundary conditions as given by (2.2).

Here we have two smooth steady state solutions,

$$\begin{aligned} u^+ &= \sin x \\ u^- &= -\sin x. \end{aligned} \tag{3.2a}$$

There is also an infinite number of possible discontinuous solutions of the form

$$\begin{aligned} u &= u^+ \qquad x < x_S \\ u &= u^- \qquad x > x_S \end{aligned}, \tag{3.2b}$$

where x_S, the "shock" location, is an arbitrary point in the interval $(0,\pi)$. Note that, in the steady state, the "shock" speed $u_S = (u^+ + u^-)/2$ is zero for any $0 < x_S < \pi$ and, therefore, (3.2b) is a legitimate steady state solution. In the above solutions we have already eliminated weak solutions that violate the 'entropy condition,' $u_L > u_R$.

We now ask two questions:

(i) From what class of initial conditions, if any, can either of the two smooth solutions, (3.2a), be reached and

(ii) Under what circumstances is a steady shock established and can its location be predicted?

Consider first the two questions in the particularly simple case when

$$g(x) = \beta \sin x, \tag{3.3}$$

i.e., the initial data is proportional to a smooth steady state. For $\beta > 1$, Theorem 1 will prove that the steady state is the smooth solution $u = u^+$. For $\beta < -1$, a corollary of Theorem 1 leads to $u = u^-$.

Theorem 1: The solution of equation (3.1) with boundary conditions (2.2), initial conditions (3.3) and $\beta > 1$ satisfies

$$\lim_{t\to\infty} u(x,t) = \sin x.$$

Proof: The characteristic equations resulting from (3.1) are

$$\frac{dx}{dt} = u \tag{3.4}$$

$$\frac{du}{dt} = u\frac{du}{dx} = \frac{dF}{dx}, \qquad F = \frac{1}{2}\sin^2 x; \tag{3.5}$$

Again using $\xi = \xi(x,t)$ to designate the origin of a characteristic curve passing through (x,t), we integrate (3.5)

$$\frac{1}{2} u^2 - \frac{1}{2} g^2(\xi) = F(x) - F(\xi)$$

or

$$u = \pm\left[2F(x) - 2F(\xi) + g^2(\xi)\right]^{1/2} . \tag{3.6}$$

As $t \to 0$, $\xi \to x$ and we have to choose the positive branch of (3.6) because $\beta > 1$. Thus, using $F = (1/2) \sin^2 x$,

$$u = \left[\sin^2 x + (\beta^2 - 1)\sin^2 \xi\right]^{1/2}. \tag{3.7}$$

We claim now that for t large enough there is a unique correspondence between a point (x,t) and $\xi(x,t)$. In fact, if a shock wave were to appear at a certain time $t > 0$, it will, because of (3.7), separate two positive states. The shock wave will have a positive speed, and consequently will propagate out of the domain. Therefore, for t large enough, we may substitute (3.7) into (3.4),

$$t = \int_{\xi}^{x} \frac{dy}{\left[2F(y) - 2F(\xi) + g^2(\xi)\right]^{1/2}} \tag{3.8}$$

or,

$$t = \int_{\xi}^{x} \frac{dy}{\left[\sin^2 y + (\beta^2 - 1)\sin^2 \xi\right]^{1/2}} . \tag{3.9}$$

For every $x < \pi$, the integrand in (3.9) cannot become singular except at the lower limit $y = \xi$, $\xi \to 0$. Thus, $t \to \infty$ as $\xi \to 0$ and the only possible solution for very large time is, from (3.7),

$$u \xrightarrow[t\to\infty]{} \left[2F(x) - 2F(\xi) + g^2(\xi)\right]^{1/2}_{\xi\to 0} = \left[2F(x) - 2F(0) + g^2(0)\right]^{1/2} = \sin x,$$

which completes the proof.

Corollary: Suppose that β in (3.3) satisfies $\beta < -1$, then

$$\lim_{t\to\infty} u(x,t) = -\sin x.$$

Note that in view of (3.8) the results of Theorem 1 hold for any initial conditions $g(x)$, such that $g(0) = 0$, $g(x) > \sin x$. The corollary is thus also extended for any $g(x) < -\sin x$.

Still continuing with the case of $g(x) = \beta \sin x$, we now consider

$$0 < \beta < 1. \tag{3.10}$$

Here the steady state will be of the form (3.2b). We will show, however, in Theorem 2 that the shock location depends on the initial condition.

Theorem 2: The solution of equation (3.1) with boundary conditions (2.2), initial conditions (3.3) and $0 < \beta < 1$ satisfies

$$\lim_{t\to\infty} u(x,t) = \begin{cases} u^+ = \sin x; & 0 < x < x_s \\ u^- = -\sin x; & x_s < x < \pi \end{cases} \tag{3.11}$$

where

$$x_s = \pi - \sin^{-1}\sqrt{1-\beta^2} > \frac{\pi}{2}. \tag{3.12}$$

Proof: From the characteristic equation (3.5), with $0 < \beta < 1$, we get

$$u(x,t) = \pm[\sin^2 x - (1-\beta^2)\sin^2(\xi(x,t))]^{1/2}. \tag{3.13}$$

In the interval $(\pi - x_s, x_s)$, x_s as defined in (3.12), $u(x,t)$ cannot change sign because the radical in (3.13) cannot vanish in said interval. Since as $t \to 0$, $u(x,t)$ is positive, we conclude that

$$u(x,t) = [\sin^2 x - (1-\beta^2)\sin^2(\xi(x,t))]^{1/2}, \quad \pi - x_s < x < x_s. \tag{3.14}$$

In this interval the first characteristic equation (3.4) becomes

$$t = \int_{\xi}^{x} \frac{dy}{[\sin^2 y - (1-\beta^2)\sin^2(\xi(x,t))]^{1/2}} \tag{3.15}$$

since $t > 0$ we must have $\xi < x$ when $\pi - x_s < x < x_s$. As $t \to \infty$, $\xi(x,t)$ must therefore vanish in the limit. It is thus established that

$$\lim_{t\to\infty} u(x,t) = \sin x, \qquad (\pi - x_s < x < x_s). \tag{3.16}$$

Next consider the interval $[0, \pi - x_s)$. Formally as $t \to \infty$, in this leftmost interval, $\xi(x,t)$ must converge either to zero or π. However, any characteristic passing through (x,t) in the interval $[0, \pi - x_s)$ cannot emanate from any $\xi > x_s$ because this would mean a negative slope, and hence

a negative u in the interval $(\pi-x_s, x_s)$; this contradicts (3.16). Having established that $\lim_{t\to\infty} \xi(x,t) = 0$, we notice that formally it is possible for a characteristic curve, originating in the interval $[0,\pi-x_s)$, to start with a positive slope (required as $t \to 0$) and change slope in the interval. This, however, will result in a solution containing a "shock" that violates the 'entropy condition' $u_L > u_R$. We thus have our next intermediate result

$$\lim_{t\to\infty} u(x,t) = \sin x, \qquad (0 \leq x < x_s). \tag{3.17}$$

It now remains for us to show that in the interval $x_s < x \leq \pi$ the solution must be negative and hence equal to $-\sin x$.

Consider

$$\frac{\partial}{\partial t}\int_0^\pi u\,dx = \frac{1}{2}\left[u^2(0,t) - u^2(\pi,t)\right]. \tag{3.18}$$

From (3.13) it follows that $u(0,t) = u(\pi,t) = 0$ (in contrast to the case of $\beta > 1$, see (3.7)). Thus

$$\int_0^\pi u(x,t)dx = \int_0^\pi u(x,0)dx = 2\beta, \tag{3.19}$$

or, as $t \to \infty$

$$\int_0^{x_s} \sin x\,dx + \lim_{t\to\infty} \int_{x_s}^\pi u(x,t)dx = 2\beta.$$

Performing the integration we find

$$\lim_{t\to\infty} \int_{x_s}^\pi u(x,t)dx = \beta - 1 < 0. \tag{3.20}$$

Consider once again (3.15). We see that as $t \to \infty$, ξ must go either to zero or π. The limit $\xi(0,\infty) \to 0$ will always result in a positive $u(x,t)$ which is contradicted by (3.20). Therefore, in (3.13) we must choose the negative sign, so

$$\lim_{t\to\infty} u(x,t) = -\sin x, \qquad (x_s < x \leq \pi). \tag{3.21}$$

This completes the proof.

Corollary: Under the conditions of Theorem 2 except that

$$-1 < \beta \leq 0$$

the solution still retains the form of (3.11) except that now

$$x_s = \sin^{-1}\sqrt{1-\beta^2} < \frac{\pi}{2}\,. \tag{3.22}$$

For arbitrary initial data the general behavior is that described in Theorems 1 and 2 and their corollaries, i.e., one can get either solution (3.2a) or (3.2b). If a "shock" is present in the steady state, the upper and lower bounds for its location are given, for $g(x) > 0$, as follows:

$$\pi - \sin^{-1}\sqrt{\sin^2 z - g^2(z)} \leq x_s \leq \pi - \sin^{-1}\sqrt{1 - \frac{1}{4}\left(\int_0^\pi g(\eta)d\eta\right)^2}\,, \tag{3.23}$$

where z maximizes the expression $\sin^2 x - g^2(x)$. For negative initial data the bounds are

$$\sin^{-1}\sqrt{\sin^2 z - g^2(z)} \leq x_s \leq \sin^{-1}\sqrt{1 - \frac{1}{4}\left(\int_0^{\pi} g(\eta)d\eta\right)^2} \,. \qquad (3.24)$$

The upper bound reflects the "area rule" (see (3.18)). The lower bound is the first point where $u(x,t)$ can change sign. For $g(x) > 0$, the upper bound becomes sharp (i.e., equals x_s), if $u(\pi,t) = 0$ for all t.

3.1 NUMERICAL RESULTS FOR THE SECOND EXAMPLE

3.1.1 Explicit Form

Equation (3.1) is discretized using the explicit E-O scheme given by equation (2.20). Numerical calculations were performed for initial conditions given by

$$g(x) = \beta \sin x, \qquad (3.25)$$

where β is a free parameter such that $0 \leq \beta \leq 1$. The steady state shock position as a function of β is plotted in Figure 5. The numerical results are in excellent agreement with the theoretical prediction given by equation (3.12). For any $\beta > 1$, the steady state obtained was u^+ given by equation (3.2a).

If one uses an algorithm employing central space differencing (e.g., MacCormack's scheme), it is then necessary to supply a numerical boundary condition. If the steady state value is used for the boundary condition, then

the numerical algorithm, though stable, fails to converge to steady state. The reason is clearly due to the fact that the numerical boundary condition does not allow for a flux through that boundary. As a consequence we have (see (3.19))

$$\int_0^\pi u(x,t)dx = 2\beta$$

for all t, while the true steady state, u^+, requires

$$\lim_{t\to\infty} \int_0^\pi u(x,t) = 2.$$

3.1.2 Implicit Form

Equation (3.1) is discretized using the implicit E-O scheme given by equation (2.28). Once again, numerical calculations were performed for initial conditions given by equation (3.25). Now, an additional free parameter is

$$\varepsilon = \frac{100}{\pi}\frac{\Delta x}{\Delta t} \tag{3.26}$$

which is a measure of how big Δt is taken in the numerical calculations. The results of these series of calculations are given in Figure 6. As indicated in the figure, if "small" Δt's are taken ($\varepsilon \geq 1/2$), then the steady state shock location calculated agrees with the theoretical prediction of equation (3.12). However, as Δt increases, the steady state shock position is found to the right of its theoretical location. For sufficiently high values of Δt (small ε's), the smooth solution is obtained.

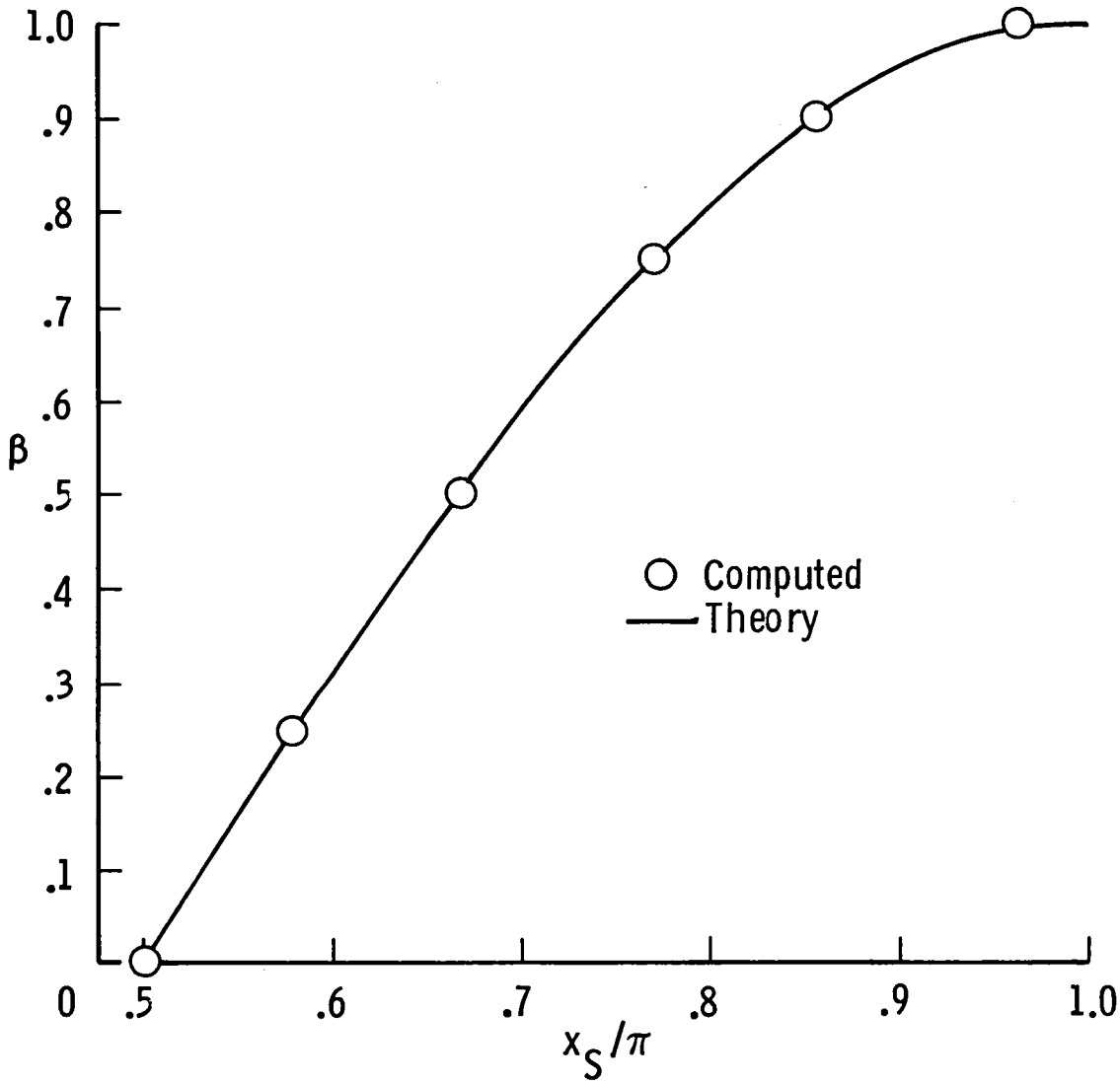

Figure 5. Computed and predicted steady state shock position for equation (3.1) with initial conditions (3.25) using a time accurate scheme.

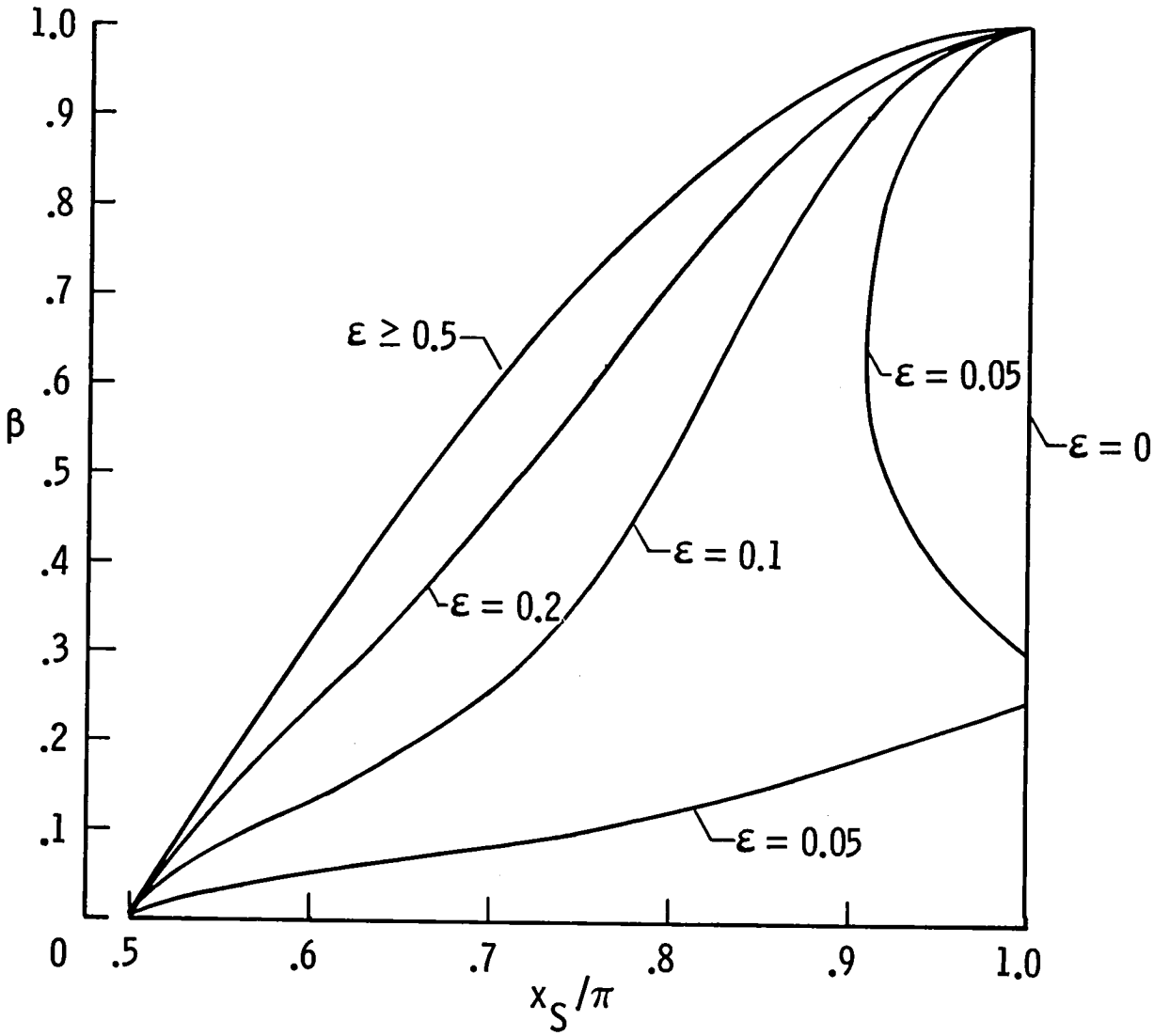

Figure 6. Computed and predicted steady state shock position for equation (3.1) with initial conditions (3.25) using an implicit scheme.

4. A MODEL FOR QUASI-ONE-DIMENSIONAL FLUID DYNAMICS

A characteristic boundary value problem, where boundary conditions are of the form (2.2), occurs in a double-throat Laval nozzle

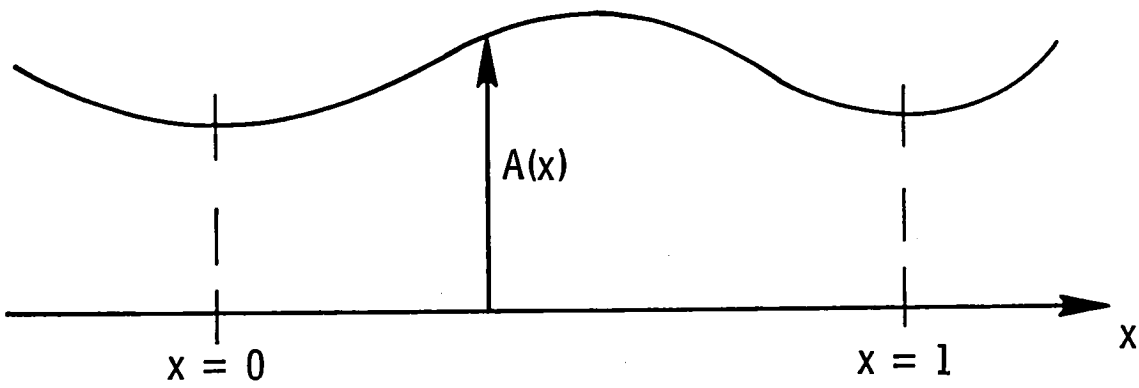

Figure 7. Sketch of double-throat nozzle

as shown in Figure 7. It is well known [1] that there are two possible smooth steady solutions, with sonic conditions at the throats. Between the throats, $0 < x < 1$, the flow can be either completely subsonic or supersonic, the exact Mach number distribution, in each case, being dependent on the nozzle area, $A(x)$.

If one considers the isentropic case only, then the flow may be described by the quasi-one-dimensional partial differential equations for the Riemann variables,

$$\psi = u + \frac{2}{\gamma - 1} c, \qquad \phi = u - \frac{2}{\gamma - 1} c,$$

where u is the velocity, $c = (\gamma p/\rho)^{1/2}$ is the speed of sound, and γ is the ratio of specific heats for ideal gases. The equations are:

$$\frac{\partial \psi}{\partial t} + (u + c)\frac{\partial \psi}{\partial x} + ucF'(x) = 0, \tag{4.1}$$

$$\frac{\partial \phi}{\partial t} + (u - c)\frac{\partial \phi}{\partial x} - ucF'(x) = 0, \tag{4.2}$$

where $F'(x) = dF(x)/dx = d\big(\ell nA(x)\big)/dx$. This is a hyperbolic system whose time evolution is difficult to describe analytically. We therefore seek a model for this system, so that with a single equation the most salient features are retained. We will present numerical evidence that analytical predictions resulting from this model equation agree very well with results found by numerical integration of the original system (4.1), (4.2).

The model is derived using a single assumption, namely that the total enthalpy is constant not only at steady state but also during the transient phase. The mathematical expression of this assumption is:

$$\phi^2 + \psi^2 + \frac{2(1 - a)}{a}\phi\psi = \frac{4c_*^2}{2a - 1} = \frac{16}{\gamma^2 - 1}c_0^2 \tag{4.3}$$

where

$$a = \frac{\gamma + 1}{4}, \tag{4.4}$$

c_0 is the stagnation sound speed, and c_* is the sonic sound speed, i.e., c_* is the sound speed at a sonic throat.

We now face the choice of solving (4.3) for either ψ in terms of ϕ, or vice versa. This dilemma is resolved by recognizing that our "physical"

problem will impose characteristic boundary conditions on (4.2), and we would like our model equation to retain this feature. Therefore, (4.2) is the relevant equation. Solving for ψ,

$$\psi = -\frac{1-a}{a} + \frac{1}{a}\left[\frac{4a^2c_*^2}{2a-1} - (2a-1)\phi^2\right]^{1/2}, \tag{4.5}$$

where the positive branch was chosen in order to satisfy the steady state boundary condition at $x = 0$, i.e., at the first throat, where:

$$\psi_* = \frac{2a}{2a-1}\,c_*; \qquad \phi_* = -\frac{2(1-a)}{2a-1}\,c_*. \tag{4.6}$$

Using (4.5) in (4.2), and defining

$$\hat{\phi} = \phi/\psi_* \tag{4.7}$$

the equation takes the form

$$\frac{\partial\hat{\phi}}{\partial\tau} + \Lambda(\hat{\phi})\,\frac{\partial\hat{\phi}}{\partial x} = H(\hat{\phi})F'(x) \tag{4.8}$$

where

$$\Lambda(\hat{\phi}) = \hat{\phi} + \frac{1-a}{\sqrt{2a-1}}\,\sqrt{1-\hat{\phi}^2} \tag{4.9}$$

$$H(\hat{\phi}) = \frac{2a-1}{4a}\left[1 - 2\hat{\phi}^2 - \frac{2(1-a)}{\sqrt{2a-1}}\,\hat{\phi}\,\sqrt{1-\hat{\phi}^2}\right] \tag{4.10}$$

$$\tau = tc_*. \tag{4.11}$$

Notice that the time scale, τ, is determined by the sonic conditions.

For the sake of clarity let us first examine the simple case of $a = 1$ ($\gamma = 3$), which corresponds to the flow of products caused by detonating solid explosives. Equation (4.8) then becomes

$$\frac{\partial \hat{\phi}}{\partial \tau} + \hat{\phi} \frac{\partial \hat{\phi}}{\partial x} = \frac{1}{4} (1 - 2\hat{\phi}^2)F'(x); \quad F(x) = \ell nA(x). \tag{4.12}$$

A smooth steady state solution of (4.12) with $\hat{\phi}(0) = 0$ is

$$\hat{\phi}^2(x) = \frac{1}{2} \left(1 - e^{-F(x)}\right), \tag{4.13}$$

and so, as in (3.2a) we have two possible steady states; one is positive (supersonic), and the other is negative (subsonic):

$$\hat{\phi}^+ = \left(\frac{A(x) - 1}{2A(x)}\right)^{1/2} \tag{4.14}$$

$$\hat{\phi}^- = - \left(\frac{A(x) - 1}{2A(x)}\right)^{1/2}. \tag{4.15}$$

Bearing in mind the results of the previous sections, we will show that in the time evolution problem, $\hat{\phi}^+$ and $\hat{\phi}^-$ are reachable from different initial conditions. Clearly, (4.14) and (4.15) can be connected by a steady shock - and again, because of the symmetry of $\hat{\phi}^+$ and $\hat{\phi}^-$, the steady shock location could be anywhere in the interval (0,1). We will show that here too bounds on x_s can be found and compare them with results of numerical integration of the original system (4.1), (4.2).

We will concentrate on the positive branch (4.14), showing that if the initial condition is given by

$$\hat{\phi}(x,0) = g(x) = \beta\hat{\phi}^{+} = \beta\left[\frac{A(x) - 1}{2A(x)}\right]^{1/2} \tag{4.16}$$

with

$$1 < \beta^2 < \frac{A_{max}}{A_{max} - 1}\ , \tag{4.17}$$

where A_{max} is the maximum area in the nozzle, then $\lim_{t\to\infty} \hat{\phi}(x,t) = \hat{\phi}^{+}(x)$. A solution of the second characteristic equation,

$$\frac{d\hat{\phi}}{d\tau} = \hat{\phi}\,\frac{d\hat{\phi}}{dx} = \frac{1}{4}\left(1 - 2\hat{\phi}^2\right)F'(x) \tag{4.18}$$

is given by

$$\left|1 - 2\hat{\phi}^2\right| = \left|1 - 2g^2\left(\xi(x,\tau)\right)\right| A\left(\xi(x,\tau)\right)/A(x), \tag{4.19}$$

where as before $\xi(x,\tau)$ is the origin of a characteristic curve passing through (x,τ). Since we have chosen (see (4.17)) $g^2(x)$ to be smaller than $1/2$, then it follows from (4.19) that

$$\hat{\phi}(x,\xi) = \pm\left[\frac{A(x) - A(\xi)\left[1 - 2g^2(\xi(x,\tau))\right]}{2A(x)}\right]^{1/2}\ , \tag{4.20}$$

where $\xi(x,\tau)$ is to be determined from the first characterisitc equation

$$\tau = \int_{\xi}^{x} \frac{dy}{\hat{\phi}(y,\xi)}\ . \tag{4.21}$$

From (4.16) we see that a positive (negative) β will initially select a positive (negative) branch of (4.20). By an argument similar to that used in Theorem 1, it remains for us to show that $\hat{\phi}$ thus initiated will not change sign while evolving to steady state. This follows immediately from (4.20) if we use for $g(x)$ equation (4.16) with $\beta > 1$.

Next we consider the discontinuous steady state solution. The initial data are now taken so that $|g(x)| < \hat{\phi}^+$, see equation (4.14). A lower bound for x_s is found by inquiring about the zeros of (4.20) - the argument is the same as in the previous section. This happens when

$$A(x_s) = A(z)\left(1 - 2g^2(z)\right) \tag{4.22}$$

where, as before, z maximizes the expression $A(x)(1 - 2g^2(x))$. To find the upper bound we have to devise an "area rule" for equation (4.12). Because of the structure of the right-hand side of (4.12), it is no longer $\int_0^1 \hat{\phi}(x,\tau)dx$ which is conserved. To find the appropriate "area rule," we divide both sides of (4.12) by $1 - 2\hat{\phi}^2 > 0$. The resulting equation after integration by x over the interval may be written as:

$$\frac{\partial}{\partial\tau}\int_0^1 \ell n\,\frac{1+\sqrt{2\hat{\phi}}}{1-\sqrt{2\hat{\phi}}}\,dx - \frac{1}{\sqrt{2}}\int_0^1 \frac{\partial}{\partial x}\left[\ell n(1-2\hat{\phi}^2)\right]dx = \frac{1}{\sqrt{2}}F(x)\Big|_0^1 = 0. \tag{4.23}$$

Under the usual area rule assumptions, $\hat{\phi}(0,\tau) = \hat{\phi}(1,\tau) = 0$, we have

$$\int_0^1 \ell n\,\frac{1+\sqrt{2}\,\hat{\phi}}{1-\sqrt{2}\,\hat{\phi}}\,dx = \text{const.} \tag{4.24}$$

Therefore, an upper bound for x_s is found from:

$$\int_0^{x_S} \ell n \frac{1+\sqrt{2}\,\hat{\phi}^+}{1-\sqrt{2}\,\hat{\phi}^+}\,dx + \int_{x_S}^{1} \ell n \frac{1+\sqrt{2}\,\hat{\phi}^-}{1-\sqrt{2}\,\hat{\phi}^-}\,dx = \int_0^1 \ell n \frac{1+\sqrt{2}\,g(x)}{1-\sqrt{2}\,g(x)}\,dx. \qquad (4.25)$$

When $g(x) \leq \beta\hat{\phi}^+$, $(\beta < 1)$ we expect, as in the previous example, the upper and lower bounds on x_S to coincide. This was indeed verified in numerical experiments with a particular area distribution, A(x).

Recalling that (4.12) is a scalar model equation representing the systems (4.1), (4.2), we find it interesting to note that this 2×2 system also possesses an area rule, namely:

$$\frac{\partial}{\partial t}\int (\psi+\phi)dx = \frac{1}{2}\left[\left(\psi^2(1,t) + \phi^2(1,t)\right) - \left(\psi^2(0,t) + \phi^2(0,t)\right)\right]. \qquad (4.26)$$

Under the assumption that $\phi(0,t) = \phi(1,t) = 0$; $\psi(0,t) = \psi(1,t)$, we have

$$\frac{\partial}{\partial t}\int (\psi + \phi)dx = 0. \qquad (4.27)$$

We can now use this to test the "goodness" of our model by comparing the shock location predicted from (4.25) with that of the system, whose solution is found numerically. This comparison is carried out in the next section.

Having concluded the analysis of the $a = 1$ case, let us now return to the more general formulation (4.8). In particular, let us consider the case of $\gamma = 1.4$ $(a = .6)$, corresponding to air. We next show how (4.8) may be cast in a form similar to the "decoupled" one in (4.12). Multiply both sides of (4.8) by $r'(\phi)$ $(r' = dr/d\phi)$:

$$\frac{\partial r}{\partial \tau} + r\frac{\partial r}{\partial x} = \frac{H(\hat{\phi}(r))}{\hat{\phi}'(r)}F'(x) = K(r)(r_+ - r)(r - r_-)F'(x), \qquad (4.28)$$

where

$$K(r) = \frac{\sqrt{1 - \frac{5}{9} r^2}\,(\sqrt{1 - \frac{5}{9} r^2} - \frac{2}{3} r)(r - \sqrt{\frac{3}{10}})(r + \sqrt{\frac{3}{2}})}{(1 - r^2)(r - \frac{3}{5}\sqrt{1 - \frac{5}{9} r^2})(\frac{5}{3} r + 5\sqrt{1 - \frac{5}{9} r^2})} \tag{4.29}$$

$$r_+ = \sqrt{\frac{3}{2}}\,, \qquad r_- = -\sqrt{\frac{3}{10}}\,. \tag{4.30}$$

The quantities r_- and r_+ are the values of r which, in the steady state, correspond to Mach numbers of zero and infinity, respectively. For general values of γ, $K(r)$, r_+ and r_- are replaced by $K(r,a)$, $r_+(a)$, $r_-(a)$. $K(r,a)$ will have the same structure as in (4.29).

It is easy to verify that $K(r)$, given by (4.29), is a positive, slowly monotonically decreasing function in the relevant range $r_- \leq r \leq r_+$. In fact $K(r_-) \approx 2K(r_+) = .309$. In the case of $\gamma = 3$, i.e., equation (4.12), $r = \phi$ and we have $r_+ = -r_- = 1/\sqrt{2}$ and $K(r) =$ constant. It is thus clear that the topological behavior of (4.28) is the same as that of (4.12), and the arguments carry over. In particular the non-unique smooth steady states depend on the initial data in the same fashion with respect to β.

4.1 NUMERICAL RESULTS FOR QUASI ONE-DIMENSIONAL EQUATIONS

Here, we study numerically equations (4.1) and (4.2) for $\gamma = 3$, namely:

$$\frac{\partial \psi}{\partial t} + \frac{\partial}{\partial x}\left(\frac{\psi^2}{2}\right) = -\frac{1}{4}\,(\psi^2 - \phi^2)F'(x) \tag{4.31}$$

$$\frac{\partial \phi}{\partial t} + \frac{\partial}{\partial x}\left(\frac{\phi^2}{2}\right) = \frac{1}{4}\left(\psi^2 - \phi^2\right)F'(x). \tag{4.32}$$

The area of the dual-throat nozzle is defined by

$$A(x) = \frac{(1 - d)^2 + \left(1 - d(2x - 1)^2\right)^2}{2(1 - d)\left(1 - d(2x - 1)^2\right)^2}, \qquad 0 \leq x \leq 1, \tag{4.33}$$

where d is a parameter related to the maximum area by

$$A_{max} = \frac{(1 - d)^2 + 1}{2(1 - d)}. \tag{4.34}$$

For the numerical experiments, we have used $d = 1/6$ which results in $A_{max} = 1.1$. The steady state Mach number distribution is

$$M(x) = A(x) \pm \sqrt{A^2(x) - 1}, \tag{4.35}$$

and the steady state solution to (4.31) and (4.32) as a function of the Mach number is

$$\psi = \sqrt{3}\,(1 + M)/(1 + M^2)^{1/2} \tag{4.36}$$

$$\phi = -\sqrt{3}\,(1 - M)/(1 + M^2)^{1/2}. \tag{4.37}$$

With the stagnation pressure and density used as reference values, the value of ψ_* is $\sqrt{6}$.

4.1.1 Explicit Form

Equations (4.31) and (4.32) are discretized using the explicit E-O scheme given by equation (2.20). Numerical calculations were performed with initial conditions corresponding to

$$\phi(x,0) = \beta \sqrt{6} \left[\frac{A(x) - 1}{2A(x)}\right]^{1/2}, \tag{4.38}$$

which is equivalent to (4.16), and with

$$\psi(x,0) = \sqrt{6} \left[\frac{A(x) + 1}{2A(x)}\right]^{1/2}, \tag{4.39}$$

or

$$\psi(x,0) = \sqrt{6} \left(1 - \beta^2 \left(\frac{A(x) - 1}{2A(x)}\right)\right)^{1/2} . \tag{4.40}$$

The initial conditions given by (4.39) correspond to the exact, steady solution for ψ; while those given by (4.40) correspond to conditions for ψ consistent with (4.38) and constant total enthalpy, (4.5). The steady state reached was the name in either case; therefore, the results reported here are for calculations with (4.40) only.

Figure 8 summarizes the numerical results. The figure compares the predicted steady state shock position as given by (4.25) for the model equation (4.12) and the computed position for the system (4.31) and (4.32). As is evident from the figure, the agreement is very good.

4.1.2 Implicit Form

Equations (4.31) and (4.32) are discretized using the implicit E-O scheme given by equation (2.28). Equations (4.38) and (4.40) are again used as initial conditions. The numerical results are summarized in Figure 9. As shown in the figure, the steady state shock position depends on the Courant number as measured by the parameter

$$\varepsilon = 100 \frac{\Delta x}{\Delta t} . \tag{4.41}$$

For values of $\varepsilon \geq 10$ the steady state shock position is the same as that predicted by the explicit form. For values of $\varepsilon < 10$ (large Δt), the steady state shock position bifurcates at certain values of β.

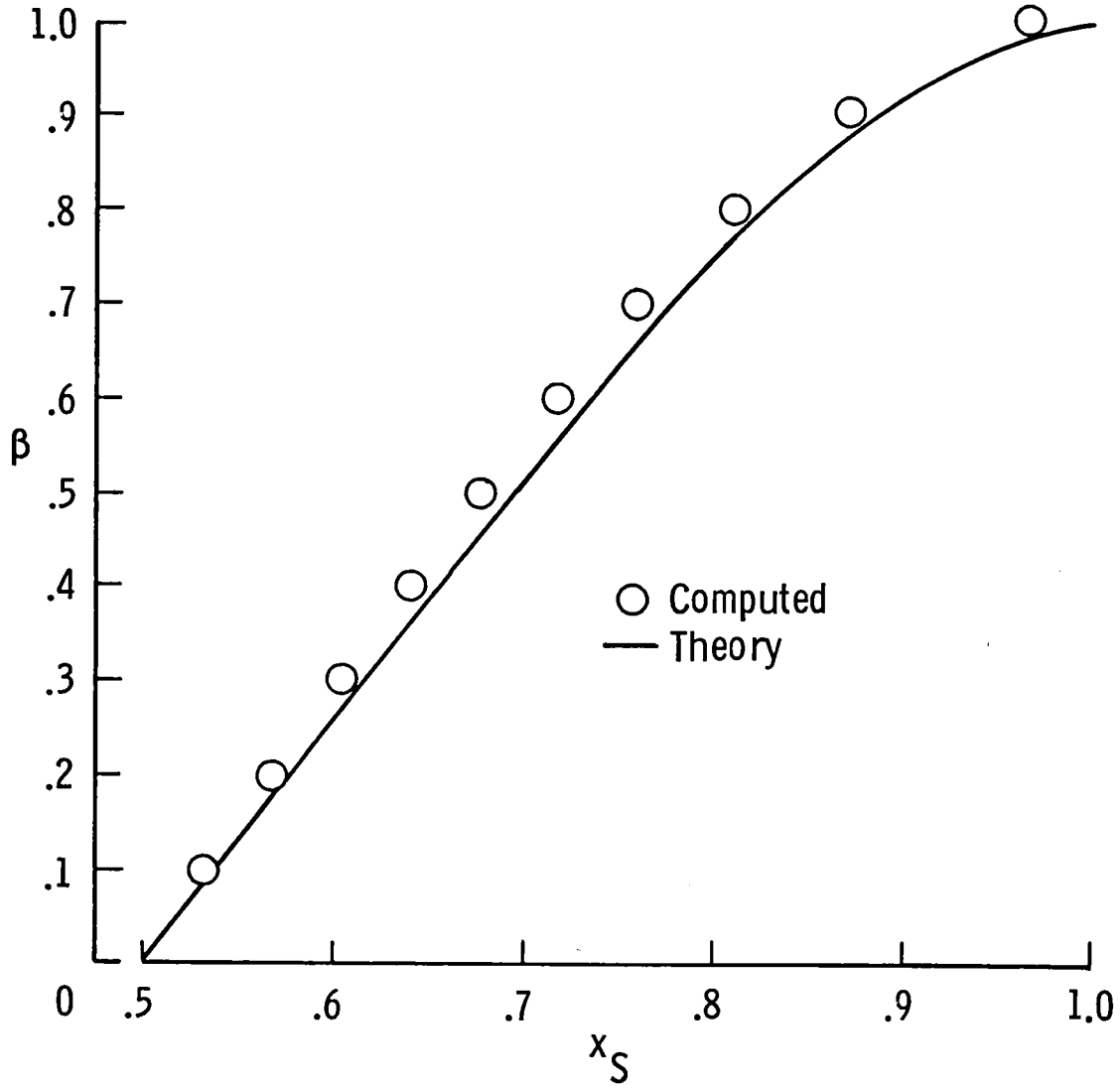

Figure 8. Predicted steady state shock position given by (4.25) for equation (4.12) and computed position for system (4.31) and (4.32) with initial conditions (4.38) and (4.40) using a time accurate scheme.

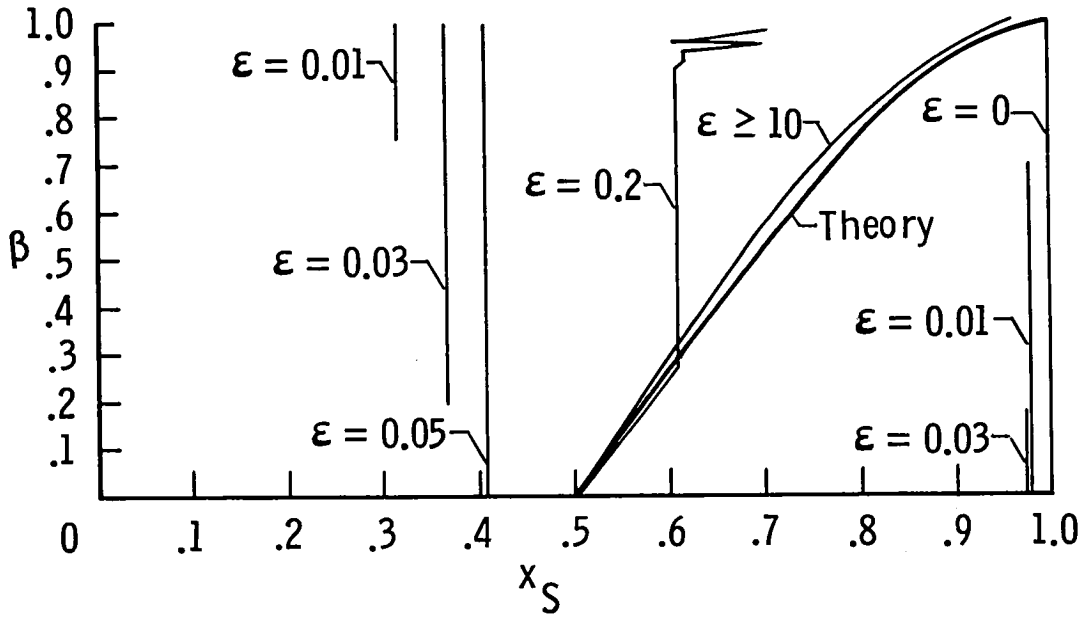

Figure 9. Predicted steady state shock position given by (4.25) for equation (4.12) and computed position for system (4.31) and (4.32) with initial conditions (4.38) and (4.40) using an implicit scheme.

CONCLUSIONS

In this paper we analyzed several model equations for characteristic initial boundary value problems and examined numerically these as well as the quasi-one-dimensional isentropic Euler equations of gas dynamics.

We show that because of the characteristic nature of the boundary conditions the resulting steady states, whether smooth or discontinuous, depend on the initial data. Different initial conditions may yield different steady states. We also gave an example (see Section 2) of solution to the steady state equation which cannot evolve from the initial data. Thus from the point of view of the time-dependent equation, we find there are no non-unique steady states.

Another conclusion that one may draw is that in order to have complete confidence in the results, numerical schemes for characteristic initial boundary value problems should be time consistent and employ only suitable boundary conditions. Thus we have shown that implicit methods, even for finite Courant numbers, may yield solutions which are piecewise combinations of non-unique solutions of the steady state equations. In fact, such numerically implicit algorithms may converge to solutions which also include parts of unstable steady states.

REFERENCES

[1] Crocco, Luigi, "One-Dimensional Treatment of Steady Gas Dynamics" in Fundamentals of Gas Dynamics, Vol. III of High Speed Aerodynamics and Jet Propulsion, Howard W. Emmons, ed., New Jersey, (1958), pp. 183-186.

[2] Embid, P., Goodman, J. and Majda, A., SIAM J. Sci. Stat. Comp., Vol. 5, No. 1 (1984), pp. 21-41.

[3] Engquist, B. and Osher, S., Math. Comp., Vol. 34, (1980), pp. 45-75.

1. Report No. NASA CR-172486 ICASE Report No. 84-57	2. Government Accession No.	3. Recipient's Catalog No.
4. Title and Subtitle MULTIPLE STEADY STATES FOR CHARACTERISTIC INITIAL VALUE PROBLEMS		5. Report Date November 1984 6. Performing Organization Code
7. Author(s) M. D. Salas, Saul Abarbanel and David Gottlieb		8. Performing Organization Report No. 84-57 10. Work Unit No.
9. Performing Organization Name and Address Institute for Computer Applications in Science and Engineering Mail Stop 132C, NASA Langley Research Center Hampton, VA 23665		11. Contract or Grant No. NAS1-17070 13. Type of Report and Period Covered Contractor Report
12. Sponsoring Agency Name and Address National Aeronautics and Space Administration Washington, D.C. 20546		14. Sponsoring Agency Code 505-31-83-01

15. Supplementary Notes

Langley Technical Monitor: J. C. South, Jr.
Final Report

16. Abstract

The time dependent, isentropic, quasi-one-dimensional equations of gas dynamics and other model equations are considered under the constraint of characteristic boundary conditions. Analysis of the time evolution shows how different initial data may lead to different steady states and how seemingly anamolous behavior of the solution may be resolved. Numerical experimentation using time consistent explicit algorithms verifies the conclusions of the analysis. The use of implicit schemes with very large time steps leads to erroneous results.

17. Key Words (Suggested by Author(s)) initial value problem, multiple steady state, characteristic boundary conditions shock waves	18. Distribution Statement 02 - Aerodynamics 64 - Numerical Analysis Unclassified - Unlimited

19. Security Classif. (of this report) Unclassified	20. Security Classif. (of this page) Unclassified	21. No. of Pages 44	22. Price A03

For sale by the National Technical Information Service, Springfield, Virginia 22161

NASA-Langley, 1984